C. R. Chimie 18 (2015) 1335–1343

Contents lists available at ScienceDirect

Comptes Rendus Chimie

www.sciencedirect.com

Full paper/Mémoire

Influence of the size and the morphology of ZnO nanoparticles on cell viability

Otilia Ruxandra Vasile [a], Ioana Serdaru [a], Ecaterina Andronescu [a], Roxana Trușcă [b], Vasile Adrian Surdu [a], Ovidiu Oprea [a], Andreia Ilie [a], Bogdan Ştefan Vasile [a,*]

[a] National Research Centre for Micro and Nanomaterials, Faculty of Applied Chemistry and Materials Science, University Politehnica of Bucharest, Science, Polizu Street No. 1-7, Bucharest 011061, Romania
[b] METAV Research and Development, No. 31 C.A. Rosetti Street, Bucharest 020011, Romania

ARTICLE INFO

Article history:
Received 30 March 2015
Accepted after revision 31 August 2015

Keywords:
Cytotoxicity
Nanopowders
TEM
ZnO
Cell viability

ABSTRACT

Zinc oxide has attracted wide research interest due to its unique properties. Its band gap width, high refractive index, high electrical conductivity, and high optical transmission in the visible, etc., have made it suitable for a variety of applications, such as gas sensors, varistors, optoelectronic devices, etc. The first part of the paper presents three methods for the synthesis of zinc oxide nanoparticles: sol–gel, polyol, and hydrothermal methods. Then, we report on the characteristics of the powders in terms of structure, composition and morphology as well as of in-vitro testing on cell cultures. The influence of the nanoparticles on cell viability was evaluated by the lactate dehydrogenase method. It turns out that all ZnO powders tested present high cytotoxicity. Also, it is found that the synthesis method significantly influences cell viability, the lowest one being obtained for nanopowders synthesized by the sol–gel method.

1. Introduction

Nanostructured materials have received increased attention due to their good and improved physical and chemical properties. Currently, nanostructured metal oxides are extremely used; their possible applications include catalysts [1,2], sensors [3], environmental remediation applications [4–6], medicine [7], solar cells [8,9], cosmetics, and personal care products [10,11].

A promising approach is the use of metal oxide nanoparticles for applications in health care (hyperthermia, drug delivery) [12]. The interest in the study of nanostructured materials is mainly due to the ease of modifying the physical properties by varying the shape and size of the particle. The properties of a material are controlled by the physical interactions and chemical composition, structure and method of synthesis [13].

Despite the many advantages of the wide applications of ZnO particles, nanomaterials may cause serious environmental and health problems [14–17], and as a consequence, the risk of human exposure increases [18].

Several studies report on ZnO material-mediated cytotoxicity. ZnO nanomaterials used in different products are identified in several organs after usage. The cytotoxicity of ZnO is also due to its increased solubility, and, as a consequence, high concentrations of nanoparticles in the environment and food chain may affect human health.

Some of these studies indicated that the toxicity of ZnO nanoparticles may be partially due to their induced cellular

* Corresponding author.
E-mail address: bogdan.vasile@upb.ro (B.Ş. Vasile).

http://dx.doi.org/10.1016/j.crci.2015.08.005
1631-0748/

oxidative stress through the generation of free radicals and reactive oxygen species (ROS). ROS are derived from mitochondria and endoplasmic reticulum. Lactate dehydrogenase is a cytoplasmic enzyme found in all cells that can be released into the extracellular medium when the cell membrane is damaged. It has been proved that LDH distribution was significantly altered by metabolic stress and that ZnO nanoparticles increase LDH activity in cells [19]. More LDH was released from cells when they were exposed to higher concentrations of ZnO NPs [20].

The release of Zn^{+} ions from the nanoparticles, due to the instability of ZnO NPs [21] in the acidic compartment of lysosomes, increases ROS generation [22,23].

Regarding the toxicity of Zn ion, nano-ZnO and bulk ZnO, some studies showed that added soluble Zn exhibited greater toxicity, while the adversely effects of nano-ZnO and bulk ZnO were caused by soluble Zn resulting from particle dissolution. In this way, soluble Zn was more toxic than nano-ZnO, while nano-ZnO was more toxic than bulk ZnO in all tested biological reactions [24].

However, contradictory results have been noted in recent studies, due to the possibility of size-dependent toxicity, distinct from adverse effects associated with the presence of dissolved ions. Metal ions released by ZnO material contributed to toxicity, but did not cause the main lethal mechanism of ZnO NPs and bulk ZnO material [15].

One study shows that ZnO NPs toxicity on normal cells was lower than on the corresponding tumour cells and that LDH leakage reflected the damage of the cell membrane and the degree of cell necrosis. It has been revealed that the toxicity of 40-, 150-, and 350-nm ZnO particles had a smaller effect in osteoblast cancer cells (MG-63), while ZnO microparticles had been less toxic. Likewise, ZnO particles of different sizes induced slightly different toxicity, so the particles' shape may influence the material's toxicity. Also, dissolved Zn^{2+} plays an important role in the toxic effect of ZnO particles [25].

Based on the toxicological aspects of bio-nanotechnology in relation to the presence of nanoscale entities in the human body and the consequences of transporting and interacting with tissues and organs [26], we report in the present study the synthesis of zinc oxide nanoparticles by hydrothermal, sol–gel and polyol methods. The obtained powders were characterized in terms of thermal stability, structure, composition and morphology, through thermal analysis (TA), X-ray diffraction (XRD), scanning electron microscopy (SEM), and transmission electron microscopy (TEM). To investigate the impact of synthesized ZnO NPs on cell membrane integrity, lactate dehydrogenase leakage was assessed after cells had been incubated with synthesized ZnO samples. The results indicated that exposure to ZnO NPs increases LDH leakage as a function of concentration and time [16].

By comparing all three synthesized ZnO powders, our toxicity results indicated that ZnO NPs high toxicity on tumoral cells is also induced by particle size, which argues that the dissolution of Zn^{2+} ions is dependent on the size of the particles, since it increases with the size of the particles [27,28].

2. Materials and methods

2.1. Synthesis methods

The present study was performed on ZnO nanoparticles that had been synthesized using three different techniques: sol–gel, polyol, and hydrothermal methods.

2.1.1. Sol–gel method for ZnO nanoparticles synthesis

The synthesis of zinc oxide nanoparticles using the sol–gel method was carried out as it follows: 13.5493 g zinc acetate ($C_4H_6O_4Zn{\cdot}2H_2O \geq 98\%$, Sigma-Aldrich) were used as a precursor for zinc oxide. The precursor's salt was dissolved in 31.51 mL of deionized water. Over the dissolved salt, 11.8592 g of citric acid ($C_6H_8O_7 \geq 99.5\%$ Riedel–de Haën) were added, with a molar ratio of 1:1 with respect to the cation. For gel formation, 4.5616 g of ethylene glycol was added to the precursor solution as 20 wt% in respect to the whole amount of precursors quantities used. The mixture thus obtained was stirred, allowed to gel, and then dried in an oven at 110 °C for 24 h. The obtained powders were heat treated at 460 °C in order to remove the organic residue.

2.1.2. Polyol method for the synthesis of ZnO nanoparticles

Polyol synthesis of ZnO nanoparticles was carried out as described by Chieng et al. [29]. ZnO nanoparticles were prepared by refluxing 13.5493 g of zinc acetate ($C_4H_6O_4Zn{\cdot}2H_2O \geq 98\%$, Sigma–Aldrich) in 100 mL of ethylene glycol (EG) ($C_2H_6O_2 \geq 99.8\%$, Sigma–Aldrich) at 160 °C for 24 h. The suspension was then centrifuged at 4000 rpm for 15 min in order to obtain a white precipitate of ZnO. Afterwards, zinc oxide was washed two times with ethanol; this was followed by another centrifugation. The resulting powder was dried in an oven at 80 °C and heat treated at 380 °C.

2.1.3. Hydrothermal method

For the synthesis of ZnO using the hydrothermal method, 60 mL of an aqueous solution of zinc acetate ($C_4H_6O_4Zn{\cdot}2H_2O \geq 98\%$, Sigma–Aldrich) 0.5 M (6.5850 g) were added to 100 mL of a solution of sodium hydroxide 2 M ($NaOH \geq 99\%$, Merck) (3.2 g). The mixture thus obtained was stirred for 15 min while maintaining the pH at 12. Then, the solution was placed in an autoclave where it was kept at a constant temperature of 90 °C for 24 h. After the hydrothermal treatment, the obtained precipitate was filtered, washed with ethanol and water, and finally dried in an oven at 90 °C [30].

2.1.4. Toxicity

The experimental procedure for the toxicity test is as follows: the MG-63 line monolayer used for the test was at an approximately 70–80% confluence, this being achieved after having seeded the plates for 24 h.

For incubating the cells with the synthesized ZnO powders, the culture medium was embedded with UV-sterilized nanoparticles, at a concentration of 1 mg/mL. The medium was placed over the cells in the plate and left to incubate for 24 h in a 24-well culture plate. After the incubation period, 50 μL of the supernatant from the plate

were taken for the LDH measurements, then transferred into a 96-well plate and mixed with a reagent according to the following protocol: first, 50 μL of substrate mix reconstituted with assay buffer solution were added and incubated at room temperature in the dark for 30 min. Afterwards, a second volume of 50 μL of stop solution was added in order to measure spectrophotometrically at a wavelength of 450 nm.

When calculating viability, it is necessary to take into account the positive control and calculate cell viability values for each powder tested, based on LDH activity, as the measured absorbance of the cells incubated with the synthesized powders divided by lysed cell activity (percentage of positive control).

The results are expressed as the mean value ± SD of three individual experiments.

The positive control that was used was the MG-53 line cells incubated in the same conditions as the cells upon which the materials of interest are tested. They were incubated in a DMEM medium without FBS in order to eliminate interferences, and then they were incubated for 24 h along with the groups of cells treated with the synthesized ZnO samples.

3. Results and discussion

The obtained powders were first characterised in terms of thermal stability. We searched for the optimum heat-treatment temperature, at which all the organic residue is removed. Then the powders were characterized by means of X-ray diffraction (XRD), scanning electron microscopy (SEM) and transmission electron microscopy (TEM). Finally, the synthesized nanoparticles were tested for cell viability against MG-63 cell line.

3.1. Thermal analysis

In Fig. 1 are presented the TG-DSC curves for the ZnO-containing powders synthesized by sol–gel (1), polyol (2), and hydrothermal (3) methods.

For the powder synthesized by sol–gel method, the TG curve (Fig. 1.1) indicates a good thermal stability up to 200 °C. At this temperature, the powder starts to decompose in a rapid succession of reactions accompanied by an exothermic peak on the DSC curve. In the 200–360 °C interval, the decomposition reactions are predominant, the exothermic peaks on DSC curve being small. In the 360–460 °C interval, the combustion of the organic residues takes place, the mass change being associated with a broad, strong exothermic peak on the DSC curve. The removal of the organic part is complete at 460 °C when a ZnO nanopowder is obtained (residual mass 24.41%). The low output is typical of sol–gel syntheses where a large percentage of the compound is made of an organic part.

The powder obtained by the polyol method (Fig. 1.2) presents a mass loss of 4% up to 140 °C accompanied by a weak endothermic effect on the DSC curve. This mass loss was attributed to the elimination of water and of the solvent molecules trapped into the compound network. The resulting compound is stable up to 280 °C when a second decomposition step begins. The mass loss in this second stage is 16.61% and corresponds to the combustion of the organic part, as seen from the exothermic peak accompanying the process on the DSC curve.

The residual mass (78.22%) obtained at 380 °C consists of ZnO nanoparticles.

As it can be observed from the TG curve (Fig. 1.3), the powder obtained by the hydrothermal method is thermally stable up to 600 °C (experimental mass loss of less than 1%). Therefore, we concluded that the ZnO nanoparticles are obtained directly by this method with no further thermal treatment needed.

3.2. X-ray diffraction

X-ray diffraction (XRD) analysis was carried out on a PANalytical Empyrean Diffractometer using Cu Kα radiation (λ = 1.541874 Å), equipped with a programmable divergence slit on the incidence side and a programmable anti-scatter slit mounted on a PIXcel3D detector. The scan was done by using the Bragg–Brentanno geometry with a step size of 0.02° and a counting time per step of 25 s.

The XRD patterns for ZnO nanopowders obtained by sol–gel, hydrothermal and polyol methods are shown in Fig. 2.

All XRD patterns present peaks, which are very close to the diffraction lines for ZnO (lines (100), (002), (101), (102), (110), (103), (200), (112), (201), (004) and (202), PDF card

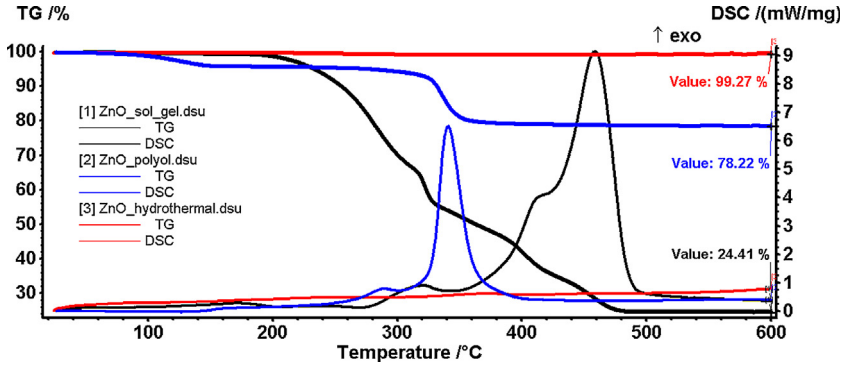

Fig. 1. (Color online.) Thermal analysis of the ZnO powders obtained by sol–gel (1), polyol (2) and hydrothermal (3) methods starting from zinc acetate as a precursor.

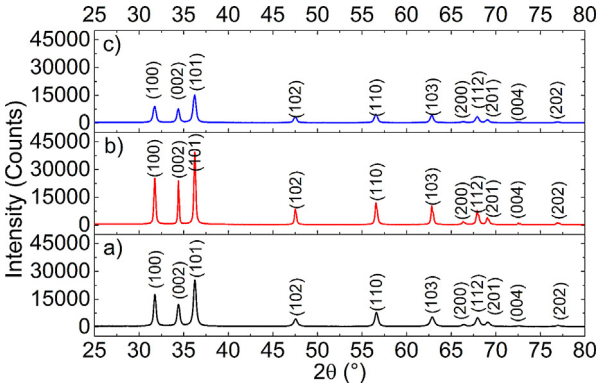

Fig. 2. (Color online.) XRD patterns obtained on: (a) ZnO powders synthesized using the sol–gel method; (b) ZnO powders obtained by the hydrothermal method and (c) ZnO powders obtained by the polyol method.

#01-080-7099). Therefore, ZnO with a hexagonal structure is identified as a single crystalline phase in all samples.

The degree of crystallinity and the average crystallite size can be estimated from the broadening of the peaks and in this case varies with the synthesis method. Thus, the highest degree of crystallinity is achieved by using hydrothermal synthesis and the lowest one for polyol synthesis.

The average crystallite size was estimated using Rietveld's full-pattern fit method. The results are presented in Table 1. The Rietveld refinement was carried out with manual background fitting and with the pseudo-Voigt profile function. The least-square refinement was converged with the $R_{expected}$, $R_{profile}$, weighted $R_{profile}$ and goodness-of-fit values presented also in Table 1, which confirm a good fit of the calculated profile function with the observed diffraction data.

The obtained data indicate that all samples have very close crystallite sizes, the biggest one being obtained for the hydrothermally synthesized one.

3.3. Scanning electron microscopy

Scanning electron microscopy images obtained on ZnO nanoparticles synthesized using sol–gel, hydrothermal and polyol methods are shown in Fig. 3 and were obtained using a Quanta inspect F Scanning electron microscope with a resolution of 1.2 nm, equipped with an EDX spectrometer from FEI (The Netherlands).

By analysing the SEM images obtained on all three samples, we can clearly see that the synthesis method has a very interesting effect on the morphology of the ZnO nanopowders starting from the same precursor. Thus, using the sol–gel method, we obtained a heterogeneous powder in terms of grain size, with very fine grains with an average size of 10–15 nm and grains of an average size of 100–150 nm. The morphology of the nanoparticles varies from small spherical particles to big polyhedral nanoparticles and even nanorods. For the hydrothermal method, a plate-like morphology of the nanoparticles is achieved, with a width of approximately 18 nm in average and a length ranging from 150 to 400 nm. The most interesting aspect of the nanopowders synthesized through the hydrothermal method is that the nanoplates are in fact transparent. Finally, using the polyol method, we obtained a very homogenous nanopowder in what concerns particle size and morphology; thus, we have synthesized spherical nanoparticles with an average grain size of approximately 15–20 nm.

Table 1
Average crystallite size.

Synthesis method	Sol-gel	Hydrothermal	Polyol
Crystallites average size (nm)	19.70 ± 3.05	22.20 ± 1.85	18.59 ± 0.64
Agreement indices			
$R_{expected}$	5.6913	3.3259	5.8003
$R_{profile}$	6.4905	6.9711	4.6652
Weighted $R_{profile}$	8.5204	9.1783	5.8541
Goodness of fit	2.2413	4.6155	2.0187

3.4. Transmission electron microscopy

Transmission electron microscopy images of the ZnO nanopowders were obtained using a Tecnai G^2 F30 S-TWIN Transmission Electron Microscope with 1-Å resolution, fully analytical, equipped with EDX and EELS spectrometers and with a STEM detector. The operating voltage of the microscope was 300 kV. The bright-field (BFTEM), high-resolution (HRTEM) images with the selected area electron diffraction patterns (SAED) and particle size distribution are presented in Figs. 4 and 5.

Bright-field transmission electron microscopy images (BFTEM) for the sol–gel synthesized nanopowder reveal particles with various shapes and sizes, with spherical to rod-like shapes. The average particle size is of 38.77 ± 1.67 nm, as it can be observed in Fig. 4g. The particle size distribution for the sol–gel-synthesized nanopowder is monomodal, with a maximum at around 33 nm. Also, by analysing the BFTEM images, we can see that the particles have the tendency to form hard agglomerates, due to the calcinations. As regards the hydrothermally synthesized nanopowder, we can see that the particles have a plate-like shape, with a diameter of 161.77 ± 7.71 nm as it can be seen in Fig. 4h and a thickness of 10–18 nm. These nanoparticles, synthesized using the hydrothermal method, are obtained individually, there is no agglomeration present.

For the polyol-synthesized nanopowder, the BFTEM images presented show nanoparticles with an average particle size of 23.31 ± 0.07 nm, with a monomodal distribution, with a maximum at 22.5 nm. The polyol method induces the formation of polyhedron-shaped nanoparticles, with almost no agglomeration. The insets in the BFTEM images represent the selected area diffraction patterns obtained on synthesized ZnO nanoparticles. All images show the formation of ZnO with a wurtzite crystal structure.

The difference observed for the crystallite size measured from XRD data and the particle size obtained from TEM bright-field data can be attributed to the fact that the particles are formed from more than one crystallite [12]. The biggest difference can be seen in the case of hydrothermally synthetized nanoparticles. For the case of polyol synthetized nanoparticles, the average nanoparticle

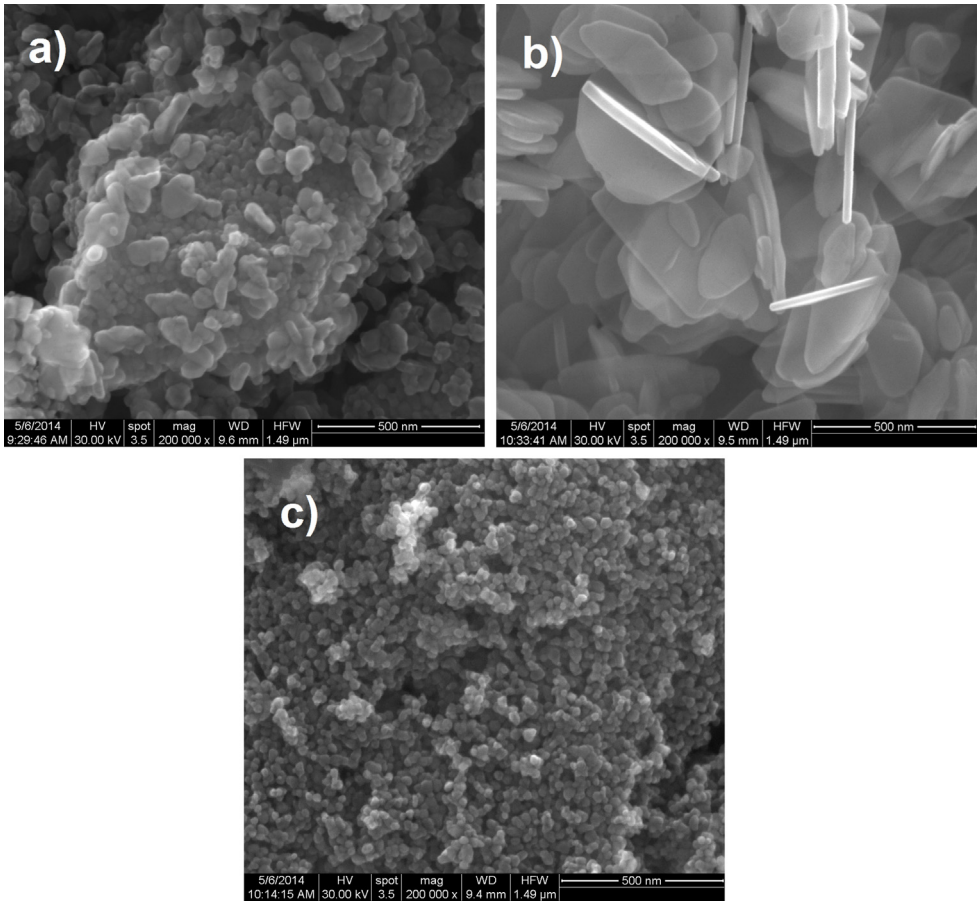

Fig. 3. SEM images obtained on: (a) ZnO powders synthesized using sol–gel method; (b) ZnO powders obtained by the hydrothermal method and (c) ZnO powders obtained by the polyol method.

size is almost the same as the crystallite size, which means that the particles are monocrystalline.

High-resolution images (HRTEM) reveal, for all methods, well-crystallized particles in which we can clearly identify the orientations with the Miller indices (002) and (100), corresponding to the interplanar distances with $d = 2.6$ Å and $d = 2.81$ Å. Also, by analysing these images, we can observe that for the polyol-synthesized nanoparticles, there is some amorphous phase present at the edge of the particles.

3.5. Cytotoxic evaluation of ZnO nanoparticles

The microscopic evaluation of the morphology and viability of MG-63 cell line in the presence of the synthesized ZnO powders was performed using the lactate dehydrogenase method (LDH). Lactate dehydrogenase is a cytosolic enzyme that is released into the culture medium as a result of the loss of cellular integrity, which results either from apoptosis or necrosis. The LDH enzyme catalyses the conversion of pyruvic acid into lactic acid, this being the marker for cellular toxicity in the biocompatibility test. LDH activity can be used as an indicator of the integrity of the cell membrane and serves as a general method for the assessment of cytotoxicity resulting from chemical compounds or toxic environmental factors. The cytotoxicity study was based on a colorimetric method that measures the amount of lactate dehydrogenase released into the environment by the lysed cells, based on the study of the enzymatic reaction, which takes 30 min. The result of the conversion of the tetrazolium salt is a red formazan product. The amount of dye formed is proportional to the number of lysed cells (whose membrane has been rendered permeable) [31,32]. In order to collect the absorbance data at a visible wavelength, a 96-well Filter Max F5, Multi-Mode Microplate reader from Molecular Devices was used.

The results demonstrate that the exposure of the MG-63 cell line to zinc oxide powders obtained from zinc acetate using the sol–gel, hydrothermal and polyol methods, at a concentration of 0.5 mg/mL for 24 h, leads to an increase in the LDH activity by decreasing the viability percentage in the range from 21 to 46%.

The images of phase-contrast microscopy at a 20 × magnification show a decrease in the viability of the cells treated with the ZnO powder and a modification of the cell morphology in respect to the untreated ones, as displayed in Figs. 6 and 7, and this is due to the presence of the ZnO powder tested in the immediate vicinity.

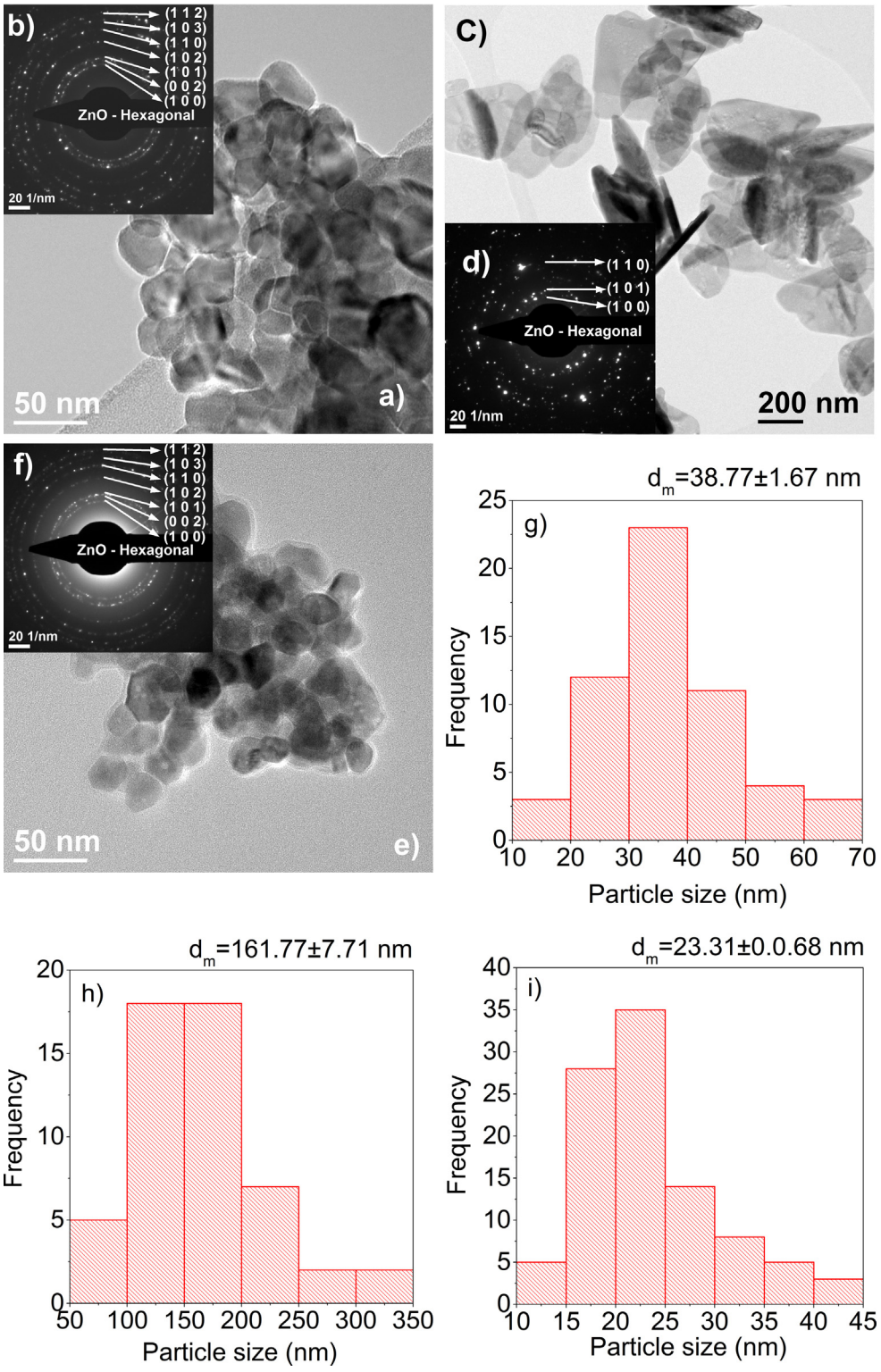

Fig. 4. (Color online.) TEM images (a), inset SAED, (b) and particle size distribution (g) obtained on a ZnO powder synthesized using the sol–gel method, TEM images (c), inset SAED (d) and particle size distribution (h) obtained on a ZnO powder synthesized using the hydrothermal method, TEM images (e), inset SAED (f) and particle size distribution (i) obtained on a ZnO powder synthesized using the polyol method.

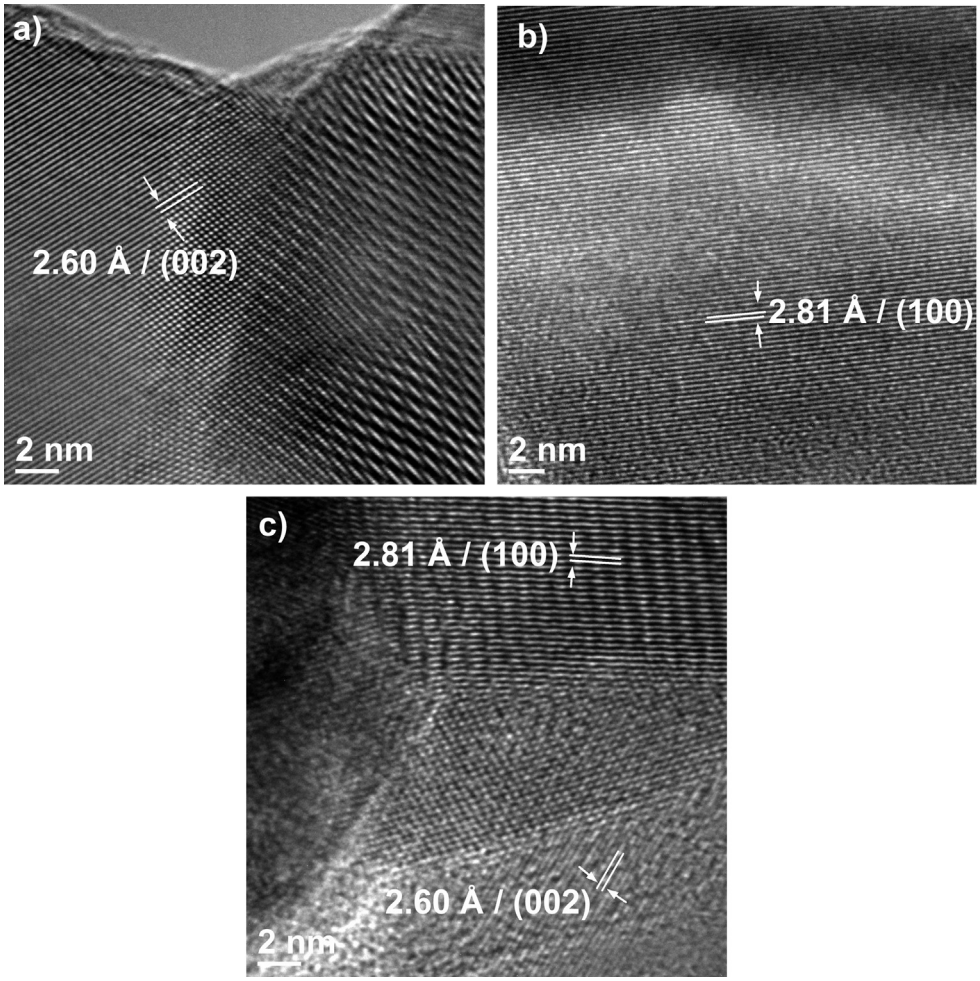

Fig. 5. HRTEM images of ZnO powder synthesized using (a) sol–gel method, (b) hydrothermal method and (c) polyol method.

The results confirmed that exposure of the MG-63 cell line to the ZnO powder obtained using the hydrothermal method, with a concentration of 0.5 mg/mL, for 24 h leads to an increased LDH activity, by decreasing the viability to 21% compared with untreated cells.

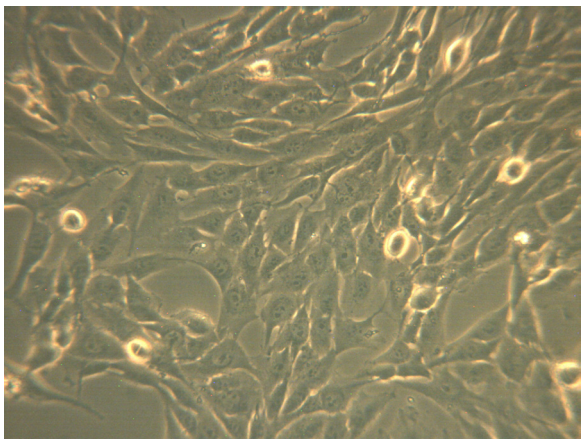

Fig. 6. (Color online.) The microscopic images in phase-contrast for osteosarcoma human cell culture corresponding to untreated cells.

Compared with zinc oxide powder obtained using the sol–gel method, it is found that the percentage of viability is only 5% lower; however, it appears that the toxicity of the powder is greatly increased, the cells are largely affected by apoptosis, and cell organelles debris is present in the environment as a cluster.

Exposure for 24 h of the MG-63 cell line to zinc oxide powder obtained using the polyol method, having a concentration of 0.5 mg/mL, leads to an increased LDH activity, by decreasing the viability to 46% compared to untreated cells.

It is noted that in the case of cells treated with zinc oxide obtained by the polyol method, the viability of the cells is also reduced, indicating a reduced biocompatibility of the powder, its cytotoxicity being higher compared to that of cells treated with the previous materials.

A moderate toxicity of the tested ZnO powders is found both in qualitative analysis microscopy, namely phase-contrast and morphological changes of the treated cells. The analysis was made by comparison the number of viable cells when incubating with other materials of

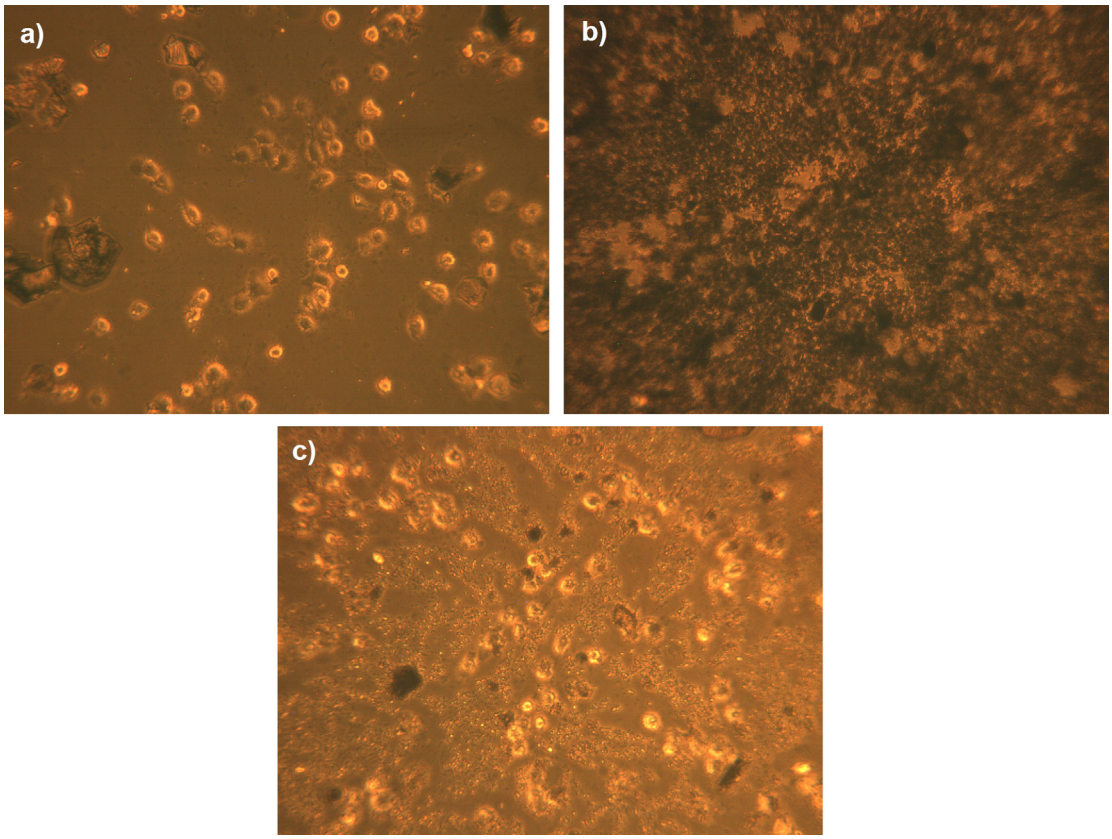

Fig. 7. (Color online.) Phase-contrast optical microscopy images for Human osteosarcoma cell culture treated with zinc oxide nanoparticles synthesized using: (a) the sol–gel method; (b) the hydrothermal method, and (c) the polyol method.

interest. The second one is quantitative analysis, since we have obtained a moderate viability of the cell line that has been subjected to testing.

The results of viability assays obtained for synthesized and characterized ZnO powders are compared in Fig. 8.

It appears that high toxicity on tumoral cells is similar for all the ZnO powders tested. Also, it is found that this is significantly influenced by the method of synthesis. Thus, the highest cytotoxicity is obtained for cells incubated with a powder synthesized by the hydrothermal method. A possible explanation may be the presence of unreacted precursors. By comparing all three synthesized ZnO powders, from the viability assay it could be seen that high toxicity is also induced by the type of the material.

From the images obtained through phase-contrast microscopy, it was found that for a concentration of 0.5 mg/mL and a time of 24 h, viable cells are present, as confirmed by quantitative analysis, but it is clear that the remaining cells are also affected, as confirmed by the sudden change in their morphology, starting from the incubation with ZnO powders.

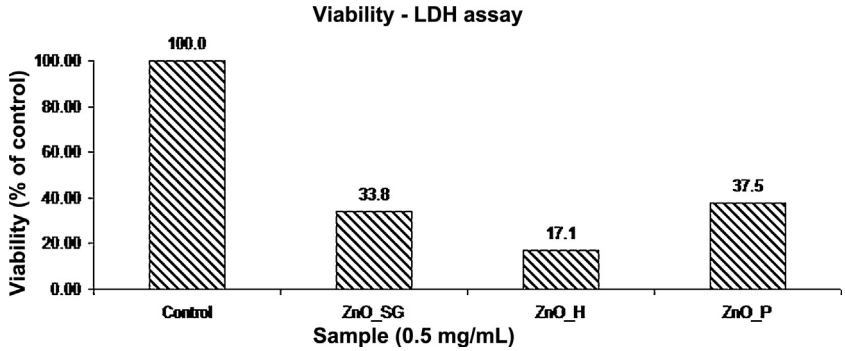

Fig. 8. Viability assay obtained for the synthesized ZnO nanopowders.

4. Conclusion

The purpose of this study was to investigate the cytotoxicity of zinc oxide nanopowders synthesized by three methods (sol–gel, hydrothermal and polyol) using zinc acetate as a precursor.

The characterization of the obtained powders was performed using X-ray diffraction, scanning electron microscopy and transmission electron microscopy. The X-ray diffraction spectra indicate that the hexagonal zinc oxide is obtained as a single-crystal phase.

Scanning electron microscopy and transmission electron microscopy showed that the obtained nanoparticles have different shapes, depending upon the method of synthesis; therefore, there are small particles of spherical shape in range of 10 to 12 nm, and large ones having a polyhedral shape. The hydrothermal method yielded particles in the form of nanostructured wafers.

The study included an evaluation of the interaction between nanoparticles and cell culture and a research of the influence of nanoparticles on cell viability by using the lactate dehydrogenase method. By comparing all three synthesized ZnO powders, from the viability assay, it could be seen that high toxicity on tumoral cells is induced by particle size. This is due to the fact that, as stated by George et al. [33], ZnO toxicity is caused by the dissolution and subsequent release of the Zn^{2+} ions, which are toxic, into the aqueous culture medium. The dissolution of Zn^{2+} ions is dependent on the size of the particles, increasing with the size of the particles [34]. This effect is also seen in our case, as the smallest particles obtained using the polyol method induced the lowest level of cytotoxicity, whereas the hydrothermally obtained ZnO particles, with larger particle sizes, induced the highest level of cytoxicity.

Acknowledgments

This work is supported by the Sectorial Operational Programme Human Resources Development, financed from the European Social Fund, and by the Romanian Government under the contract number ID 134398 (KNOWLEDGE).

References

[1] L. Zhang, N. Li, H. Jiu, G. Qi, Y. Huang, Ceram. Int. 41 (2015) 6256.
[2] C. Mateos-Pedrero, H. Silva, D.A. Pacheco Tanaka, S. Liguori, A. Iulianelli, A. Basile, A. Mendes, Appl. Catal., B 174–175 (2015) 67.
[3] Y.R. Wong, Y. Yuan, H. Du, X. Xia, Sens. Actuators, A 229 (2015) 23.
[4] M. Tan, G. Qiu, Y.P. Ting, Bioresour. Technol. 185 (2015) 125.
[5] H. Ma, P.L. Williams, S.A. Diamond, Environ. Pollut. 172 (2013) 76.
[6] S. Bandyopadhyay, G. Plascencia-Villa, A. Mukherjee, C.M. Rico, M. José-Yacamán, J.R. Peralta-Videa, J.L. Gardea-Torresdey, Sci. Total Environ. 515–516 (2015) 60.
[7] H. Zhang, B. Chen, H. Jiang, C. Wang, H. Wang, X. Wang, Biomaterials 32 (2011) 1906.
[8] K. Poornima, K. Gopala Krishnan, B. Lalitha, M. Raja, Superlattices Microstruct. 83 (2015) 147.
[9] J. Qi, W. Liu, C. Biswas, G. Zhang, L. Sun, Z. Wang, X. Hu, Y. Zhang, Opt. Commun. 349 (2015) 198.
[10] C.L. Kuo, C.L. Wang, H.H. Ko, W.S. Hwang, K. Chang, W.L. Li, H.H. Huang, Y.H. Chang, M.C. Wang, Ceram. Int. 36 (2010) 693.
[11] T.H. Le, A.T. Bui, T.K. Le, Powder Technol. 268 (2014) 173.
[12] O.R. Vasile, E. Andronescu, C. Ghitulica, B.S. Vasile, O. Oprea, E. Vasile, R. Trusca, J. Nanopart. Res. 14 (2012) 1269.
[13] O. Oprea, O.R. Vasile, G. Voicu, E. Andronescu, I. Craciun, DJNB 7 (2012) 1757.
[14] R. Roya, M. Das, P.D. Dwivedi, Toxicological mode of action of ZnO nanoparticles: impact on immune cells, Mol. Immunol. 63 (2015) 184.
[15] D. Xiong, T. Fang, L. Yu, X. Sima, W. Zhu, Sci. Total Environ. 409 (2011) 1444.
[16] S. Seker, E. Elçin, T. Yumak, A. Sınag, Y.M. Elçin, Toxicol. In Vitro, 28 (2014) 1349.
[17] R.J. Vandebriel, W.H. De Jong, Nanotechnol. Sci. Appl. 5 (2012) 61.
[18] M. Premanathan, K. Karthikeyan, K. Jeyasubramanian, G. Manivannan, Nanomed. Nanotechnol. 7 (2011) 184.
[19] M. Pandurangan, D.H. Kim, Saudi J. Biol. Sci. (2015), http://dx.doi.org/10.1016/j.sjbs.2015.03.013.
[20] C. Wang, H. Wang, M. Lin, X. Hu, Process Saf. Environ. 93 (2015) 265.
[21] Y.Y. Kao, Y.C. Chen, T.J. Cheng, Y.M. Chiung, P.S. Liu, Toxicol. Sci. 125 (2012) 462.
[22] S. Syama, P.J. Sreekanth, H.K. Varma, P.V. Mohanan, Toxicol. Mech. Methods 24 (2014) 644.
[23] B.C. Heng, X. Zhao, S. Xiong, K.V. Ng, F.Y.C. Boey, J.S.C. Loo, Food Chem. Toxicol. 48 (2010) 1762.
[24] G. Liu, D. Wang, J. Wang, C. Mendoza, Sci. Total Environ. 409 (2011) 2852.
[25] W. Songa, J. Zhang, J. Guoa, J. Zhang, F. Ding, L. Li, Z. Sun, Toxicol. Lett. 199 (2010) 389.
[26] R. Roya, M. Das, P.D. Dwivedi, Mol. Immunol. 63 (2015) 184.
[27] E.A. Meulenkamp, J. Phys. Chem. 102 (1998) 7764.
[28] A. Aboulaich, C.M. Tilmaciu, C. Merlin, C. Mercier, H. Guilloteau, G. Medjahdi, R. Schneider, Nanotechnology 23 (2012) 335101.
[29] B.W. Chieng, Y.Y. Loo, Mater. Lett. 73 (2012) 78–82.
[30] R. Shi, P. Yang, X. Dong, Q. Ma, A. Zhang, Appl. Surf. Sci. 264 (2013) 162.
[31] F. Li, H. Liu, L. Yu, J. Nanosci. Nanotechnol. 13 (2013) 7.
[32] V. Rudic, L. Cepoi, L. Rudi, V. Miscu, T. Chiriac, A. Cojocari, D. Sadovnic, T. Guţul, A. Todosiciuc, Buletinul ASM Ştiinţele vieţii Microbiologia şi Biotehnologia 2 (2012).
[33] S. George, S. Pokhrel, T. Xia, B. Gilbert, Z. Ji, M. Schowalter, A. Rosenauer, R. Damoiseaux, K.A. Bradley, L. Mädler, A.E. Nel, ACS Nano 4 (2010) 15.
[34] A. van Dijken, E.A. Meulenkamp, D. Vanmaekelbergh, A. Meijerink, J. Phys. Org. Chem. 104 (2000) 8.